Engineering Structures 167 (2018) 431–444

Contents lists available at ScienceDirect

Engineering Structures

journal homepage: www.elsevier.com/locate/engstruct

A novel cable element for nonlinear thermo-elastic analysis

M. Rezaiee-Pajand*, M. Mokhtari, Amir R. Masoodi

Department of Civil Engineering, Ferdowsi University of Mashhad, Iran

ARTICLE INFO

Keywords:
Three-dimensional cable element
Elastic catenary
Large sag
Pretension
Thermal loading

ABSTRACT

The exact solution of inextensible catenaries in Cartesian coordinates is utilized to propose an efficient two-node cable element for static analysis of three-dimensional cable structures. This element can consider out of plane inclination without using any transformation matrices. Since the element is formulated within the framework of large curvature assumption, cables with large sag, as encountered in long-span cable-stayed bridges and suspension bridges, can be modeled accurately. The proposed element also accounts for the thermal effects. By defining the stiffness component as the ratio of infinitesimal load increment to infinitesimal increase in length, explicit entries of the tangent stiffness matrix are derived through equating the total differentiation of the strained length and the elastic elongation of the cable. The tangent stiffness matrix is available in a closed form and the need of taking the inverse of the flexibility matrix, which is faced in the solution procedure of elastic catenary, is eliminated. The robustness of the suggested technique is established through investigation of significant case studies, including slack and pre-tensioned spatial cable networks. Excellent agreement between the present results and those found in the literature indicates the versatility of the proposed scheme.

1. Introduction

Over the past two centuries, analysis and design of cable-supported structures have received huge attention as a crucial topic in the mainstream of scientific research. Owing to their unique mechanical and aesthetic features, cables are widely applied as constituent parts of many engineering structures, such as, suspension roofs, long-span suspension bridges, cable supported bridges and power transmission lines. Cables are flexible members that exhibit highly nonlinear behavior when subjected to external loads. This structure, within a cable-supported body, undergoes large displacements and rotations and sustains significant portions of load. Pretension is proposed as a simple technique to alleviate the deflection of cable structures. Numerous studies can be found in the literature addressing various schemes for investigation of the behavior of cable structures. In fact, the cable members have been widely modeled, based on two different approaches, namely the finite element method with interpolation functions and also the analytical approach which makes use of explicit expressions of a catenary.

In the first scheme, a cable is represented by a number of two-node, multi-node or generally curved elements. The displacement field within the element domain is approximated using the interpolation functions. In 1965, Ernst suggested that a cable member can be modeled by truss elements for the first time. He also introduced a modified axial stiffness to account for the sag effects of a hanging cable [1]. Although his method provided satisfactory results in some cases, it was rather inefficient since a large number of truss elements was required to achieve an acceptable level of accuracy. Later, Knudson embarked on the improvement of this method in 1971 [2]. Various researchers have further developed the truss element by introducing the nonlinear behavior and various loading conditions [3,4]. Besides, different types of two-node elements with rotational degrees of freedom have been proposed by several researchers [5–7]. The cable members have been also modeled based on the isogeometric approach with Lagrangian shape functions. In this method, the shape of an infinitesimal cable element is approximated using multi-node curved elements [8,9]. Wu and Su implemented a Four-node isogeometric element for analysis of cable structures [10]. In 2013, a six-node isogeometric element was proposed by Wang et al. [11]. The main drawback of the isogeometric elements in modeling of cable assemblies is their complexity and large number of degrees of freedom. This makes the analysis laborious and significantly time consuming. Further, since the explicit form of the tangent stiffness matrix is not available, numerical approaches must be iteratively adopted to derive the tangent stiffness matrix. In some cases, such analysis approaches lead to the numerical instabilities [12].

On the other hand, an element based on the analytical expressions of the elastic catenary was first utilized by O'brien and Francis [13]. They showed that each cable member within a cable structure can be modeled using a single analytical element. In this method, the overall equilibrium of a stretched cable element is satisfied in the Lagrangian

* Corresponding author.
E-mail address: rezaiee@um.ac.ir (M. Rezaiee-Pajand).

https://doi.org/10.1016/j.engstruct.2018.04.022
Received 18 January 2018; Received in revised form 6 April 2018; Accepted 7 April 2018

coordinates, and the exact profile is derived by imposing the boundary conditions at the end of the cable. Many researchers have developed the elastic catenary element by introducing thermal effects and different loading types [14–20]. Salehi Ahmad Abad et al. proposed an extended three-dimensional catenary element which takes the thermal effects and distributed lateral loads in different directions into account [21]. Naghavi Riabi and Shooshtari implemented the elastic catenary along with the Ramberg-Osgood stress-strain relationship to investigate the effects of material nonlinearity on the behavior of cable networks [22]. Recently, Crusells-Girona et al. have employed a mixed variational approach in curvilinear coordinates based on the elastic catenary expressions to model cables with material and geometric nonlinearity [23]. Moreover, a number of researchers have adopted the parabola approach for analysis and design of practical cable structures. Since the parabola approach disregards the large sag effects, it provides an approximate solution to the hanging cables. It is proved that the error of the method increases by increasing the sag to span ratio. Therefore, this approach is unsuitable for modeling deep cables [24–26].

In addition to the aforementioned finite element approaches, many researchers have developed innovative ways for nonlinear analysis of cable structures. Lewis employed the principle of minimum total potential energy along with the dynamic relaxation method to assess the efficiency of pure numerical approaches in analysis of pre-tensioned cable nets [27]. A two-link structure was utilized by Kwan to develop a simple technique for nonlinear analysis of pre-tensioned cable structures. In this approach, similar to a spatial truss, the nonlinear equilibrium equations were written for each node, and then, they were solved by using an iterative method [28]. Stefanou and Moossavi Nejad minimized the total potential energy of the entire structural assembly by the conjugate gradient method to obtain the equilibrium state of the cable structures [29]. The efficiency of various dynamic relaxation methods in analysis of cable structures was studied by Hüttner et al. [30]. To model single-span cables considering extensibility and thermal strains, the finite difference approach was applied by Bouaanani et al. [31,32].

Although the elastic catenary provides highly accurate results, the tangent stiffness matrix is not explicitly available. Therefore, a complicated iterative procedure must be adopted to determine the nodal forces and establish the flexibility matrix. To perform a very systematic analysis, the inverse of the flexibility matrix must be also computed to obtain the stiffness matrix. Thus, many difficulties arise during the analysis procedure of the elastic catenary. On the other hand, simplified cable approaches, such as elastic parabola or elastic straight shape, are problematic in addressing the large sag effects in the deep cables. Moreover, these elements must be transformed from a local axis to the global one via transformation matrices to be able to consider inclination. This action further increases the computational complexities. To improve these drawbacks, a three-dimensional cable element is proposed in this study for static analysis of the general cable structures. The elemental shape considers inclination without using transformation, and it takes both the large sag and thermal strain effects into account. To make the nonlinear analysis easier, the components of the tangent stiffness matrix are presented by relatively simple closed-form expressions. Since the profile of the hanging cable is given by hyperbolic functions, for convenience, the proposed element is referred to as the 'elastic hyperbola'. The numerical outcomes of the studied problems reveal the accuracy and efficiency of the present element in the nonlinear analysis of spatial cable structures.

2. Formulation of the hyperbolic cable

The configuration of a perfectly flexible and elastic cable element stretched between two nodes, namely i and j, is depicted in Fig. 1. As it can be seen, the projected lengths along the x, y and z directions are designated l_x, l_y and l_z, respectively. Further, the nodal forces and nodal displacements along the global axes, initial unstrained length and the

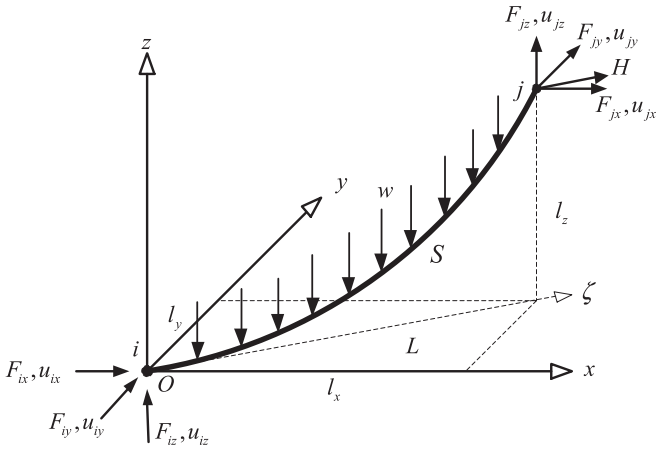

Fig. 1. Configuration of the hyperbolic cable element under self-weight.

self-weight per unit unstained length are denoted by F, u, S and w, in a respective manner.

The cross-sectional area, elastic modulus and thermal expansion coefficient of the cable are supposed to be constant, and the formulation is developed within the framework of small strains. Note that L and H correspond to the horizontal projected length and the horizontal force of the cable along the local axis, ζ, respectively. Herein, it is assumed that the profile of the cable is sufficiently deep. In other words, no limitations are imposed on the curvature of this structural element. It is worth mentioning that removal of this assumption leads to the simplified elastic parabola approach. Based on the foregoing hypotheses, the profile of the cable hanging under its self-weight with respect to the ζ axis can be defined by the following hyperbolic function [17]:

$$z(\zeta) = \frac{H}{w}\left[\cosh\left(\frac{w}{H}\zeta + \xi\right) - \cosh(\xi)\right] \tag{1}$$

It should be added that satisfaction of the boundary conditions, i.e. $z(0) = 0$ and $z(L) = l_z$, will lead to the subsequent constants:

$$\xi = \sinh^{-1}\left(\frac{\lambda l_z}{L\sinh(\lambda)}\right) - \lambda$$
$$\lambda = \frac{wL}{2H} \tag{2}$$

Another parameter is defined as $L = \sqrt{l_x^2 + l_y^2}$. It can be easily shown that the cable tension at the Cartesian coordinates has the next expression:

$$T(\zeta) = H\sqrt{1 + \left(\frac{dz}{d\zeta}\right)^2} = H\cosh\left(\frac{w}{H}\zeta + \xi\right) \tag{3}$$

where T is the tension of the cable. After deformation, the strained length of the cable element can be obtained as:

$$P = \int_0^L \sqrt{1 + \left(\frac{dz}{d\zeta}\right)^2}\, d\zeta = \sqrt{\left(\frac{L}{\lambda}\sinh(\lambda)\right)^2 + l_z^2} \tag{4}$$

where P stands for the strained length of the cable element. Since a real cable has finite axial flexibility, the inextensibility condition must be relaxed to obtain its elastic elongation. For an extensible cable with constant material properties, the Hooke's law is held:

$$\varepsilon(\zeta) = \frac{T(\zeta)}{EA} + \alpha\Delta\vartheta \tag{5}$$

where ε, E, A, α and $\Delta\vartheta$ refer to the cable strain, elastic modulus, cross-sectional area, thermal expansion coefficient and uniform variation in the temperature, respectively. Substituting for the cable tension from Eq. (3) into Eq. (5) and performing some mathematical manipulations yield:

$$d\Delta S = \frac{H}{EA}\left(1+\left(\frac{dz}{d\zeta}\right)^2\right)d\zeta + \alpha\Delta\vartheta\sqrt{1+\left(\frac{dz}{d\zeta}\right)^2}\,d\zeta \tag{6}$$

where $d\Delta S$ corresponds to an infinitesimal increment in the unstrained length of the cable. The elastic elongation of the cable element can be easily obtained by integrating both sides of Eq. (6). The solution proceeds as:

$$\Delta S = \frac{wL^2\sinh(2\lambda)}{4EA}\left[\frac{1}{2\lambda^2}+\left(\frac{l_z}{L\sinh(\lambda)}\right)^2+\frac{1}{\lambda\sinh(2\lambda)}\right] + \alpha\Delta\vartheta\sqrt{\left(\frac{L}{\lambda}\sinh(\lambda)\right)^2+l_z^2} \tag{7}$$

In which ΔS refers to the elastic elongation of the cable element. Because the strained length of the cable is equal to sum of the unstrained length and the elastic elongation, the following equality holds true:

$$P = S + \Delta S \tag{8}$$

It follows from Eq. (8) that for a given H, the unstrained length of the cable can be directly calculated. When the unstrained length of the cable element is given instead, Eq. (8) represents a nonlinear equation by which the value of the horizontal force must be determined. A simple and efficient iterative procedure, based on the modified Newton-Raphson technique, will be discussed later to handle this issue.

As it can be seen in Fig. 1, the nodal forces F_{jx} and F_{jy} represent the projected resultants of the horizontal force H along the global x and y axes. In order to derive the tangent stiffness matrix, independent of transformation matrices, the following relationships must be exploited:

$$F_{jx} = H\frac{l_x}{L} \tag{9}$$

$$F_{jy} = H\frac{l_y}{L} \tag{10}$$

Moment equilibrium in the O–ζ plane will lead to the next relationship:

$$F_{jz} = H\frac{l_z}{L} + \frac{wS}{2} \tag{11}$$

Substitution for the horizontal force by Eqs. (9)–(11) in Eqs. (4)–(7) gives rise to:

$$P_n = \sqrt{\left(\frac{L}{\lambda_n}\sinh(\lambda_n)\right)^2+l_z^2} \quad \text{for } n = x,y,z \tag{12}$$

$$\Delta S_n = \frac{wL^2\sinh(2\lambda_n)}{4EA}\left[\frac{1}{2\lambda_n^2}+\left(\frac{l_z}{L\sinh(\lambda_n)}\right)^2+\frac{1}{\lambda_n\sinh(2\lambda_n)}\right] + \alpha\Delta\vartheta P_n \quad \text{for } n = x,y,z \tag{13}$$

In which n is a dummy variable and other parameters have the following form:

$$\lambda_n = \frac{wl_n}{2\tau_n}, \tau_x = F_{jx}, \tau_y = F_{jy} \quad \text{and} \quad \tau_z = F_{jz} - \frac{wS}{2} \tag{14}$$

3. Derivation of the tangent stiffness matrix

In the beginning, to determine the components of the tangent stiffness matrix in an explicit manner, the following expressions are available based on Eqs. (12) and (13):

$$dP_n = \frac{\partial P_n}{\partial F_{jn}}dF_{jn} + \frac{\partial P_n}{\partial l_x}dl_x + \frac{\partial P_n}{\partial l_y}dl_y + \frac{\partial P_n}{\partial l_z}dl_z \tag{15}$$

$$d\Delta S_n = \frac{\partial \Delta S_n}{\partial F_{jn}}dF_{jn} + \frac{\partial \Delta S_n}{\partial l_x}dl_x + \frac{\partial \Delta S_n}{\partial l_y}dl_y + \frac{\partial \Delta S_n}{\partial l_z}dl_z \tag{16}$$

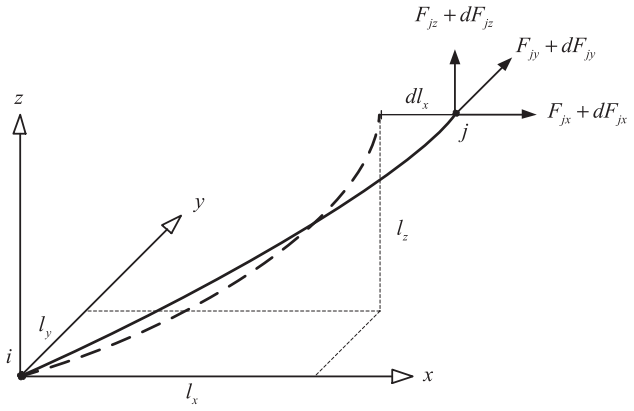

Fig. 2. Infinitesimal increase in the nodal forces due to infinitesimal increment of l_x.

Since the initial unstrained length of the cable is a constant value, its derivative equals to zero. Hence, for any n, differentiating both sides of Eq. (8) yields:

$$dP_n = d\Delta S_n \tag{17}$$

Clearly, Eq. (17) indicates that the total differentiation of the elastic elongation, and the strained length of the cable are equal. Upon substitution of Eqs. (15) and (16) into Eq. (17), the following interesting expression will be achieved:

$$\frac{\partial P_n}{\partial F_{jn}}dF_{jn} + \frac{\partial P_n}{\partial l_x}dl_x + \frac{\partial P_n}{\partial l_y}dl_y + \frac{\partial P_n}{\partial l_z}dl_z = \frac{\partial \Delta S_n}{\partial F_{jn}}dF_{jn} + \frac{\partial \Delta S_n}{\partial l_x}dl_x + \frac{\partial \Delta S_n}{\partial l_y}dl_y + \frac{\partial \Delta S_n}{\partial l_z}dl_z \tag{18}$$

Eq. (18) forms the basis for calculation of the stiffness components.

As shown in Fig. 2, assuming that an infinitesimal increment equal to dl_x is applied to node j, such that the projected length of the cable along the x direction is increase to $l_x + dl_x$. This gives rise to infinitesimal load increments, dF_{jx}, dF_{jy} and dF_{jz} in the nodal forces of F_{jx}, F_{jy} and F_{jz}. Note carefully that in such a case, dl_y and dl_z equal to zero and vanish.

Next, substituting by x for n in Eq. (18) leads to:

$$\frac{\partial P_x}{\partial F_{jx}}dF_{jx} + \frac{\partial P_x}{\partial l_x}dl_x = \frac{\partial \Delta S_x}{\partial F_{jx}}dF_{jx} + \frac{\partial \Delta S_x}{\partial l_x}dl_x \tag{19}$$

The first entry of the tangent stiffness matrix for node j, i.e. k_{11}, is defined as the ratio of the infinitesimal increment in the nodal force F_{jx} to the infinitesimal length increase dl_x [33]. Dividing Eq. (19) by dl_x and rearranging the resultant, the stiffness component can be obtained as:

$$k_{11} = \frac{dF_{jx}}{dl_x} = \frac{\frac{\partial \Delta S_x}{\partial l_x} - \frac{\partial P_x}{\partial l_x}}{\frac{\partial P_x}{\partial F_{jx}} - \frac{\partial \Delta S_x}{\partial F_{jx}}} = \frac{B_1 - A_1}{A_4 - B_4} \tag{20}$$

The tangent stiffness formulae k_{21} and k_{31} which denote the ratio of infinitesimal increment in the nodal forces F_{jy} and F_{jz} to dl_x, respectively, can be evaluated in a similar manner:

$$k_{21} = \frac{dF_{jy}}{dl_x} = \frac{\frac{\partial \Delta S_y}{\partial l_x} - \frac{\partial P_y}{\partial l_x}}{\frac{\partial P_y}{\partial F_{jy}} - \frac{\partial \Delta S_y}{\partial F_{jy}}} = \frac{B_5 - A_5}{A_8 - B_8} \tag{21}$$

$$k_{31} = \frac{dF_{jz}}{dl_x} = \frac{\frac{\partial \Delta S_z}{\partial l_x} - \frac{\partial P_z}{\partial l_x}}{\frac{\partial P_z}{\partial F_{jz}} - \frac{\partial \Delta S_z}{\partial F_{jz}}} = \frac{B_9 - A_9}{A_{12} - B_{12}} \tag{22}$$

Likewise, the rest of the stiffness components for node j can be calculated by applying infinitesimal increments to the projected length of the cable along the y and z directions and repeating the

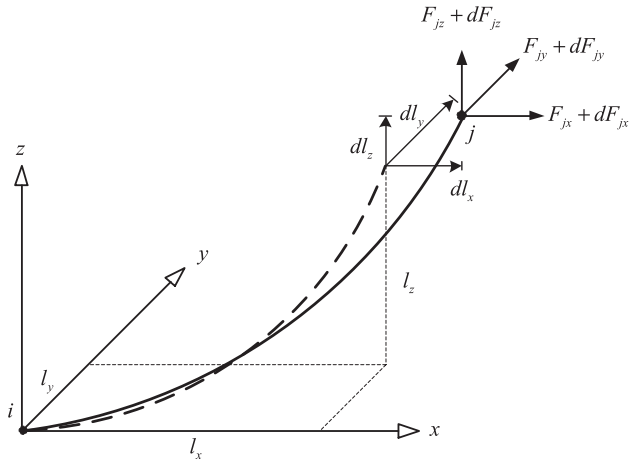

Fig. 3. Final configuration of the cable element subjected to infinitesimal length increments.

aforementioned procedure for $n = y,z$. The final configuration of the cable element is depicted in Fig. 3. The rest of the stiffness components for node j are also given below:

$$k_{12} = \frac{dF_{jx}}{dl_y} = \frac{\frac{\partial \Delta S_x}{\partial l_y} - \frac{\partial P_x}{\partial l_y}}{\frac{\partial P_x}{\partial F_{jx}} - \frac{\partial \Delta S_x}{\partial F_{jx}}} = \frac{B_2 - A_2}{A_4 - B_4} \tag{23}$$

$$k_{22} = \frac{dF_{jy}}{dl_y} = \frac{\frac{\partial \Delta S_y}{\partial l_y} - \frac{\partial P_y}{\partial l_y}}{\frac{\partial P_y}{\partial F_{jy}} - \frac{\partial \Delta S_y}{\partial F_{jy}}} = \frac{B_6 - A_6}{A_8 - B_8} \tag{24}$$

$$k_{32} = \frac{dF_{jz}}{dl_y} = \frac{\frac{\partial \Delta S_z}{\partial l_y} - \frac{\partial P_z}{\partial l_y}}{\frac{\partial P_z}{\partial F_{jz}} - \frac{\partial \Delta S_z}{\partial F_{jz}}} = \frac{B_{10} - A_{10}}{A_{12} - B_{12}} \tag{25}$$

$$k_{13} = \frac{dF_{jx}}{dl_z} = \frac{\frac{\partial \Delta S_x}{\partial l_z} - \frac{\partial P_x}{\partial l_z}}{\frac{\partial P_x}{\partial F_{jx}} - \frac{\partial \Delta S_x}{\partial F_{jx}}} = \frac{B_3 - A_3}{A_4 - B_4} \tag{26}$$

$$k_{23} = \frac{dF_{jy}}{dl_z} = \frac{\frac{\partial \Delta S_y}{\partial l_z} - \frac{\partial P_y}{\partial l_z}}{\frac{\partial P_y}{\partial F_{jy}} - \frac{\partial \Delta S_y}{\partial F_{jy}}} = \frac{B_7 - A_7}{A_8 - B_8} \tag{27}$$

$$k_{33} = \frac{dF_{jz}}{dl_z} = \frac{\frac{\partial \Delta S_z}{\partial l_z} - \frac{\partial P_z}{\partial l_z}}{\frac{\partial P_z}{\partial F_{jz}} - \frac{\partial \Delta S_z}{\partial F_{jz}}} = \frac{B_{11} - A_{11}}{A_{12} - B_{12}} \tag{28}$$

where A_i and B_i constants are used for simplification purposes, and all of them will be reported in Appendix A. At this stage, the stiffness formulae are available in a closed-form and the tangent stiffness matrix for node j can be established, as follows:

$$\mathbf{k} = \begin{bmatrix} k_{11} & k_{12} & k_{13} \\ k_{21} & k_{22} & k_{23} \\ k_{31} & k_{32} & k_{33} \end{bmatrix} \tag{29}$$

The nodal force and length increments of node j are related as:

$$\mathbf{k}\{dl_x \;\; dl_y \;\; dl_z\}^T = \{dF_{jx} \;\; dF_{jy} \;\; dF_{jz}\}^T \tag{30}$$

where k is the tangent stiffness matrix of node j and dl corresponds to the difference between the nodal incremental displacements of two nodes. The nodal displacement increments and infinitesimal length increments are related as:

$$\{dl_x \;\; dl_y \;\; dl_z\}^T = \{du_{jx} - du_{ix} \;\; du_{jy} - du_{iy} \;\; du_{jz} - du_{iz}\}^T \tag{31}$$

where du refers to the increment in the nodal displacements u. Substituting Eq. (31) into Eq. (30) and carrying out some algebra, the next result will be obtained:

$$[-\mathbf{k} \;\; \mathbf{k}]\{du_{ix} \;\; du_{iy} \;\; du_{iz} \;\; du_{jx} \;\; du_{jy} \;\; du_{jz}\}^T = \{dF_{jx} \;\; dF_{jy} \;\; dF_{jz}\}^T \tag{32}$$

The equilibrium of nodal forces within the element requires the following relation:

$$\{F_{ix} \;\; F_{iy} \;\; F_{iz}\}^T = \{-F_{jx} \;\; -F_{jy} \;\; wS - F_{jz}\}^T \tag{33}$$

Total differentiation of Eq. (33) results in the equilibrium equation for node i as:

$$[\mathbf{k} \;\; -\mathbf{k}]\{du_{ix} \;\; du_{iy} \;\; du_{iz} \;\; du_{jx} \;\; du_{jy} \;\; du_{jz}\}^T = \{dF_{ix} \;\; dF_{iy} \;\; dF_{iz}\}^T \tag{34}$$

Using Eqs. (32) and (34), the equilibrium equation of the cable element will be achieved:

$$[\mathbf{K}]\{\mathbf{dU}\}^T = \{\mathbf{dF}\}^T \tag{35}$$

In which

$$[\mathbf{K}] = \begin{bmatrix} \mathbf{k} & -\mathbf{k} \\ -\mathbf{k} & \mathbf{k} \end{bmatrix} \tag{36}$$

$$\{\mathbf{dU}\} = \{du_{ix} \;\; du_{iy} \;\; du_{iz} \;\; du_{jx} \;\; du_{jy} \;\; du_{jz}\} \tag{37}$$

$$\{\mathbf{dF}\} = \{dF_{ix} \;\; dF_{iy} \;\; dF_{iz} \;\; dF_{jx} \;\; dF_{jy} \;\; dF_{jz}\} \tag{38}$$

where **K**, **dU** and **dF** correspond to the tangent stiffness matrix of the element, incremental nodal displacement vector and incremental nodal force vector, respectively.

As a matter of fact, the tangent stiffness matrix of the proposed element given by Eq. (36) is derived with respect to the global axes, and thus a transformation matrix is not required to consider inclination. This significantly decreases the complexities and computational issues encountered in analysis of three-dimensional cable structures. The flexibility matrix of an elastic catenary is a function of three unknown nodal forces. These unknown forces must be determined through a rather complicated iterative procedure. In contrast, the stiffness matrix in Eq. (36) depends only on one unknown force, namely the horizontal force of the cable element. Hence, only a single value, i.e. the horizontal force, must be calculated at each iteration step. Contrary to the common procedures, it is not required to take the inverse of the flexibility matrix at each iteration step since the explicit tangent stiffness matrix is available and can be directly utilized. For pre-tensioned cables, the pretension force is known in place of the unstrained length. Unlike the elastic catenary that makes use of a laborious iterative procedure to determine the unstrained length, the unstrained length of the cable can be directly calculated in the present scheme by means of Eq. (8). The foregoing merits of the proposed element make it remarkably efficient in the analysis of a great variety of cable structures, including slack or pre-tensioned cable networks.

4. Nonlinear analysis process

As it was already discussed in Section 2, when the initial unstrained length of the cable is known instead of the horizontal force, the nonlinear equation given by Eq. (8) must be solved to obtain the value of H. The Newton-Raphson technique provides a simple and efficient numerical procedure to handle this problem. However, convergence to the correct solution cannot be guaranteed unless sufficient criteria are introduced into the Newton-Raphson scheme.

A schematic illustration of $f(\lambda) = P - S - \Delta S$ is depicted in Fig. 4. As it can be seen by dashed lines, the equation has three roots in terms of λ. The positive root indeed corresponds to the correct solution by which the value of H can be determined, and the two negative roots are unacceptable. Contrary to a taut cable, the Newton-Raphson technique may converge to any of these three possible solutions in case of slack cables. In order to avoid unwanted solutions, i.e. the negative roots, a constraint is built into the Newton-Raphson scheme, as discussed by Ahmadi-Kashani and Bell [16]. An initial value for λ is required to

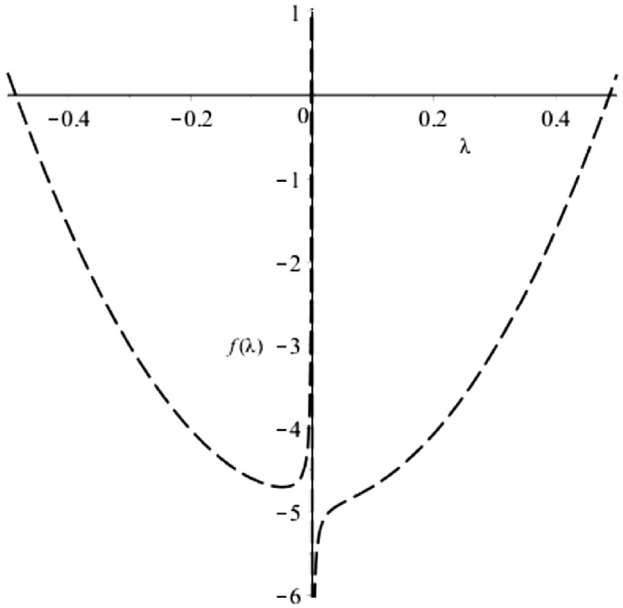

Fig. 4. Schematic view of the possible solutions for the horizontal force.

begin the iterations. This initial value may either be underestimated or overestimated. For an underestimated value, the convergence is always to the correct solution. In contrast, an overestimated initial value for λ is likely to yield a negative value for the updated λ, even in the first iteration cycle. This indeed leads to the unwanted solutions. As a remedy, wherever a negative value for λ is detected, its value is halved and used in place of the updated value obtained by the Newton-Raphson method in that iteration. Hence, the modified iterative method proceeds according to:

$$\lambda^{i+1} = \begin{cases} \lambda^i - f(\lambda^i)/f'(\lambda^i) & \text{for } \lambda^{i+1} > 0 \\ \frac{\lambda^i}{2} & \text{for } \lambda^{i+1} < 0 \end{cases} \tag{39}$$

To accelerate the Newton-Raphson procedure and converge to the required solution by fewer iterations, the initial value of λ must be chosen as close to the actual solution as possible. This further improves the numerical stability of the method. An appropriate initial value for λ can be chosen based on the following relations:

$$\lambda \approx \begin{cases} \sqrt{\sqrt{120\eta - 20} - 10} & \text{for } 1 < \eta \leqslant 3.67 \\ 2.337 + 1.095\ln(\eta) & \text{for } 3.67 < \eta \leqslant 4.5 \times 10^5 \\ -0.00473[7.909 - \ln(\eta)]^{2.46} & \end{cases} \tag{40}$$

where . If the cable is pre-tensioned, η falls outside the boundaries given by Eq. (40). In such a case, the elasticity effects cannot be neglected and a good estimate for λ may be given by $\lambda = w\sqrt{l_x^2 + l_y^2 + l_z^2}/2T$ where the approximate tension can be obtained as:

$$T \approx \begin{cases} b^{1/3} + \frac{a}{3} & \text{for } b^{1/3} > a \\ a + \frac{b}{2a^2} & \text{for } b^{1/3} \leqslant a \end{cases} \tag{41}$$

In which $a = AE\left(\frac{\sqrt{l_x^2 + l_y^2 + l_z^2} - S}{\sqrt{l_x^2 + l_y^2 + l_z^2}}\right)$ and $b = \frac{AE}{24}w^2S^2\left(\frac{l_z}{L}\right)^2$.

Since the cable structures inherently exhibit geometrical nonlinear behavior, it is necessary to implement an incremental-iterative solution method. As it is obvious, no snap-through or snap-backs are observed in analysis of cable structures and thus a load control scheme can be employed. Among the load control methods, Newton-Raphson technique has been the most popular for nonlinear structural analysis. It should be reminded that many researchers have developed and utilized this approach [34–37]. In this study, Newton-Raphson scheme is employed to trace the equilibrium paths. In this way, the governing finite element equation is obtained at time $t+\Delta t$ as below:

$$\mathbf{R}(U_{t+\Delta t}, \Gamma_{t+\Delta t}) = \Delta\Gamma_{t+\Delta t}\mathbf{F}^{ext} - \mathbf{F}^{\mathbf{int}}(U_{t+\Delta t}) \tag{42}$$

in which $\mathbf{F}^{\mathbf{int}}(U_{t+\Delta t})$ is the vector of internal forces. It is worth mentioning that these quantities are obtained based on the displacements, $\mathbf{U}_{t+\Delta t}$. Moreover, the vector of external loads is defined by $\mathbf{F}^{ext}$ and $\Delta\Gamma$ is the load factor which remains constant at all iterations of each increment. The linearized form of Eq. (42) for each iteration of increments is given by:

$$\mathbf{K}^i_{t+\Delta t}\Delta\mathbf{U}^{i+1}_{t+\Delta t} = \mathbf{R}(U_{t+\Delta t}, \Gamma_{t+\Delta t}) \tag{43}$$

where R refers to the residual force vector. In other words, external loads are computed at the first iteration of each increment and remain constant throughout the other iterations of this step. The load factor $\Delta\Gamma$ is also defined at the beginning of the analysis. The system of equations can be solved as:

$$\mathbf{K}^i_{j-1}\delta\mathbf{U}^i_1 = \Delta\Gamma\mathbf{F}^{ext} \text{for } j = 1 \mathbf{K}^i_{j-1}\delta\mathbf{U}^i_j = \mathbf{R}^i_{j-1} \text{for } \ j \geqslant 2 \tag{44}$$

The flowchart of the incremental Newton-Raphson solution procedure for nonlinear analysis of cable structures is provided in Appendix B.

5. Verification and numerical examples

In this section, various popular benchmark problems are studied to establish the efficiency and applicability of the geometric nonlinear analysis program, which is developed by authors, for using the suggested element. In case of single span hanging cables subjected to self-weight and a concentrated load at $s = s_1$, where s denotes the Lagrangian coordinate along the cable unstrained length, an analytical solution exists based on the elastic catenary expressions [38]:

$$x(s) = \frac{Hs}{EA} + \frac{H(1+\alpha\Delta\vartheta)}{w}\left[\sinh^{-1}\left(\frac{V}{H}\right) - \sinh^{-1}\left(\frac{V-ws}{H}\right)\right]$$
$$z(s) = \frac{s}{EA}\left(V - \frac{ws}{2}\right) + \frac{H(1+\alpha\Delta\vartheta)}{w}\left[\sqrt{1+\left(\frac{V}{H}\right)^2} - \sqrt{1+\left(\frac{V-ws}{H}\right)^2}\right]$$
$$for\ 0 \leqslant s \leqslant s_1 \tag{45}$$

$$x(s) = \frac{Hs}{EA} + \frac{H(1+\alpha\Delta\vartheta)}{w}\left[\sinh^{-1}\left(\frac{V}{H}\right) - \sinh^{-1}\left(\frac{V-F_c-ws}{H}\right) + \sinh^{-1}\left(\frac{V-F_c-ws_1}{H}\right) - \sinh^{-1}\left(\frac{V-ws_1}{H}\right)\right]$$
$$z(s) = \frac{s}{EA}\left(V - \frac{ws}{2}\right) + \frac{H(1+\alpha\Delta\vartheta)}{w}\left[\sqrt{1+\left(\frac{V}{H}\right)^2} - \sqrt{1+\left(\frac{V-F_c-ws}{H}\right)^2} + \frac{F_c w}{HEA}(s_1 - s) + \sqrt{1+\left(\frac{V-F_c-ws_1}{H}\right)^2} - \sqrt{1+\left(\frac{V-ws_1}{H}\right)^2}\right]$$
$$for\ s_1 \leqslant s \leqslant S \tag{46}$$

where F_c corresponds to the concentrated load at $s = s_1$ and V stands for the vertical component of the cable tension at its left end. The unknown values can be achieved by substitution of the right end boundary conditions in the second relations of Eqs. (45) and (46). These analytical expressions will be utilized for verification of the proposed element in modeling of single span deep and shallow cables.

5.1. Isolated cable subjected to concentrated load

This example presents an isolated cable with the span of 304.8 m. This problem was first considered by Michalos and Birnstiel [39] and later studied by several researchers [13–15,17–19,21,40]. The initial geometry of the cable and the necessary data for analysis are taken from [19] and presented in Fig. 5 and Table 1. The cable is hanging under its self-weight, and a concentrated force is applied at node 2. The cable was modeled using 2 elastic hyperbola elements. The displacements are compared with the previous studies and the analytical solution in

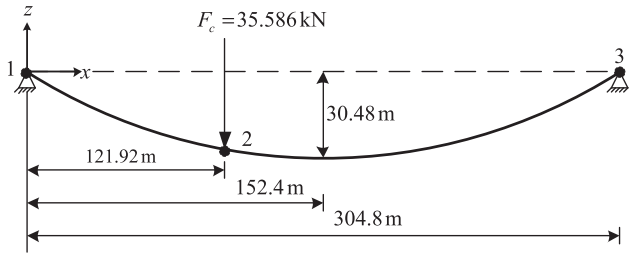

Fig. 5. Initial geometry of the isolated cable.

Table 1
Characteristics of the isolated cable.

Item	Data
Cross sectional area	548.4 mm^2
Elastic modulus	131000 MPa
Self-weight per unit unstrained length	46.12 N/m
Cable sag under self-weight at node 2	29.276 m
Unstrained length of cable element 1–2	125.847 m
Unstrained length of cable element 2–3	186.855 m

Table 2
Comparison of present and previous results for the isolated cable.

Researcher(s)	Element Type	No. of elements	Displacement at node 2 (m)	
			u_x	u_z
Saafan [40]	Truss	–	−0.845	−5.472
O'Brien & Francis [13]	Elastic catenary	2	−0.860	−5.627
Michalos & Birnstiel [39]	Truss	–	−0.845	−5.472
Jayaraman & Knudson [19]	Elastic catenary	2	−0.859	−5.626
Jayaraman & Knudson [19]	Truss	10	−0.845	−5.471
Tibert [17]	Elastic catenary	2	−0.859	−5.626
Tibert [17]	Associate catenary	2	−0.859	−5.655
Tibert [17]	Elastic parabola	2	−0.866	−5.601
Andreu et al. [14]	Elastic catenary	2	−0.860	−5.626
Yang & Tsay [15]	Elastic catenary	2	−0.859	−5.625
Thai & Kim [18]	Elastic catenary	2	−0.859	−5.626
Salehi Ahmad Abad et al. [21]	Elastic catenary	2	−0.859	−5.626
Crusells-Girona et al. [23]	Discrete elastic catenary	3	−0.861	−5.630
Present	Analytical	1	−0.859	−5.626
Present	Elastic hyperbola	2	−0.859	−5.626

Table 2. As it can be seen, the displacements obtained by the proposed element are in excellent agreement with those found in the literature. Fig. 6 depicts the comparison of the load-displacement curves for node 2 where the excellent agreement between the proposed scheme, and the elastic catenary is clearly demonstrated.

5.2. Deep cable subjected to self-weight and a temperature variation

This example serves to demonstrate the potential of the proposed element in modeling deep cables. The problem consists of a cable hanging under its self-weight which spans 100 m. Note that the supports are at the same elevation. The axial stiffness *AE*, thermal expansion coefficient and mass per unit length of the cable are equal to 5×10^4 kN, 1.25×10^{-5}K^{-1} and 25 kg/m, respectively. This cable also undergoes a temperature variation of $\Delta\vartheta = 10$ K. The cable profile is obtained for three different values of horizontal force, namely $H = 10$ kN, $H = 15$ kN, $H = 20$ kN, by using the proposed scheme and the analytical solutions given via Eqs. (45) and (46). To utilize the analytical expressions, F_c and s_1 must be set to zero. In all cases, the sag to span ratio is larger than 1: 8 and thus the cable is regarded as deep. The resulting profiles are illustrated in Fig. 7. As it can be seen, there is an excellent agreement between the proposed results and the analytical solution. This fact clearly demonstrates that authors' element is able to accurately model extensible cables with large sag. It is worth mentioning that Bouaanani and Marcuzzi [31] implemented a complicated and rather cumbersome finite difference technique to obtain the same profile whereas the present scheme readily bears the correct configuration using a single element.

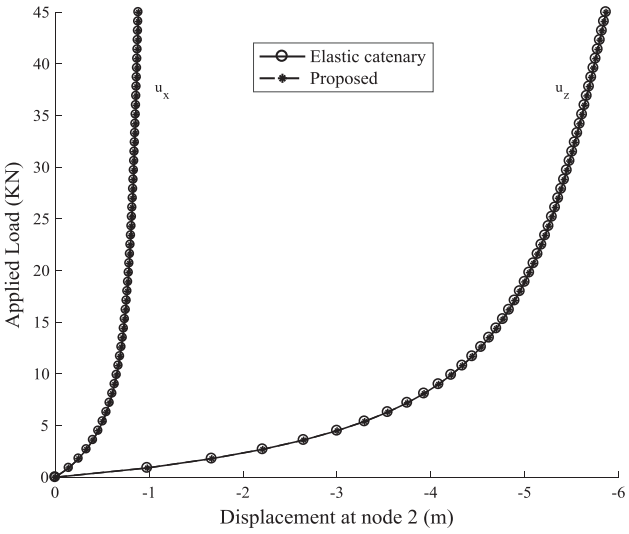

Fig. 6. Load-displacement curves for node 2.

5.3. Thermo-elastic analysis of an isolated cable

The third example is included to validate the reliability of the proposed element in the thermal analysis of cables. The problem refers to a cable the left end of which is fixed at the coordinates (0,90) m while the elevation of its right end support is kept constant at 30 m and the horizontal coordinate of the right end is varied between 0.02 and 100 m (see Fig. 8). The cable is subjected to a temperature rise of $\Delta\vartheta = 100$ K. The necessary properties of the cable are outlined in Table 3. The problem was first studied by Pevrot and Goulois [20] and later analyzed by Yang and Tsay [11] and Salehi Ahmad Abad et al. [21]. It is aimed to obtain the horizontal and vertical reactions at the right end support. To

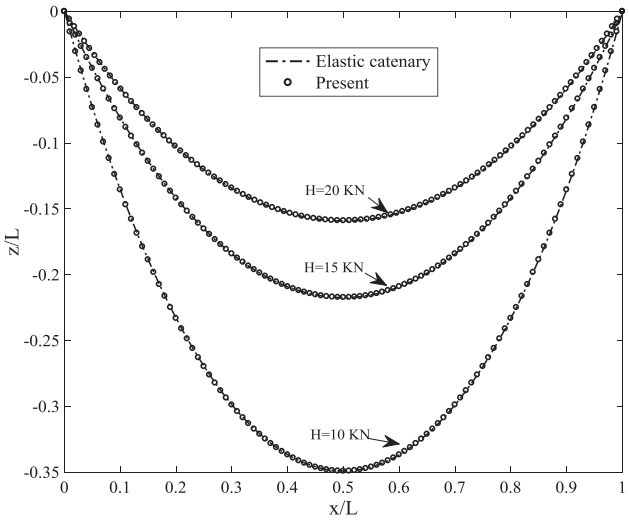

Fig. 7. Present and elastic catenary profiles of the deep cable subjected to self-weight.

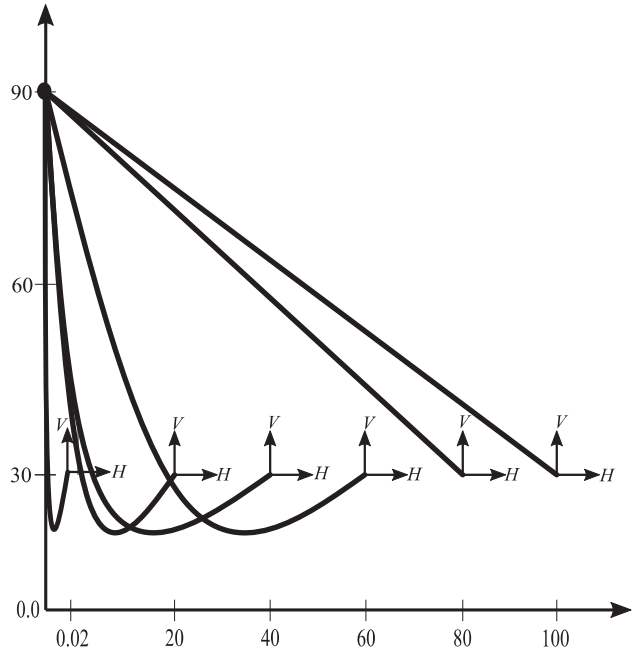

Fig. 8. Various configurations of the cable.

Table 3
Properties of the cable under thermo-elastic loading.

Item	Data
Cross sectional area	$1\,m^2$
Elastic modulus	$3 \times 10^7\,N/m^2$
Self-weight per unit unstrained length	1 N/m
Thermal expansion coefficient	$6.5 \times 10^{-6}\,K^{-1}$
Unstrained length	100 m

solve this problem, a single elastic hyperbola element was implemented in all cases. The results are compared to the literature in Table 4. As it can be seen, the proposed element has led to almost identical results with those predicted by previous researchers.

5.4. Prestressed cable under uniform load

It was observed that the present element could accurately model slack cables without difficulties. The analytical expressions of the elastic catenary are based on the flexibility concept and consistently satisfy the equilibrium of internal forces with the elastic elongation of the cable. Since the present element is directly formulated within the framework of stiffness concept, to account for the pre-elongation of a taut cable, the elasticity effects cannot be neglected and thus the cable weight per unit length must be updated as the length of the cable is increased throughout the solution process according to the following relation:

$$w^i P^i = w^0 S \tag{47}$$

where w^i and w^0 refer to the updated and initial value of the cable weight per unit length, respectively. It is clear that this equation implies the conservation of mass. Unless the proposed modification is introduced into the formulations, the distributed load of the cable will not be recomputed. This will result in larger vertical reactions and deflections than the reality. This modification has been simply built into the solution program to analyze prestressed cables.

The fourth example is presented to assess the applicability of the new formulation for analysis of a prestressed cable subjected to uniform transverse loads. The problem is taken from Jayaraman and Knudson [19]. The initial unstrained length of the cable has been 9990.00999 in. Due to pretension, the length of the cable is increased to span 10000 in, as shown in Fig. 9. It is aimed to obtain the vertical displacement at mid-span for different values of uniform transverse load. The horizontal line joining the supports has been utilized as the starting geometry. The cable was modeled by two elastic hyperbola elements. The obtained results for five different values of w are reported in Table 5. It is observed that the present results conform well to the benchmark outcomes. Fig. 10 compares the variation of mid-span displacement of the cable under increasing uniform load obtained by the proposed element and the analytical theory of elastic catenary.

5.5. Longest cable of a cable-stayed bridge

In this practical example, the proposed element is implemented to analyze the longest cable of the Sutong Changjiang high-way bridge in China. The cable is perfectly elastic with a chord length of 576.488 m and an initial unstrained length equal to 574.805 m. The cross-sectional area, elastic modulus and weight per unit unstrained length are equal to $A = 0.012046\,m^2$, $E = 190$ GPa and $w = 988\,N/m$, respectively. The coordinates of the left and right ends of the cable are given as (0, 220.564 m) and (532.626 m, 0), respectively. Since the initial unstrained length of the cable is shorter than its chord length, the strained profile of the cable represents a taut behavior. This problem was modeled only by one element. Table 6 compares the present results against the benchmarks. A good agreement is achieved once again.

5.6. Prestressed plane cable net

In this example, a prestressed plane cable net consisting of inclined and horizontal members is inspected. The geometry of the cable

Table 4
Comparison of reactions (N) for the cable under thermo-elastic loading.

Researcher(s)	Reactions (N)	Location (m)					
		0.02	20	40	60	80	100
Pevrot & Goulois [20]	*H*	0	3.061	9.172	22.15	504	4,170,000
	V	20.02	19.93	19.24	15.73	−328	−2,511,000
Yang & Tsay [15]	*H*	0.01	3.061	9.172	22.15	504.1	4,255,700
	V	20.02	19.93	19.24	15.73	−328.9	−2,555,340
Salehi Ahmad Abad et al. (DCC) [21]	*H*	0.01	3.09	9.16	22.11	504.48	4,255,849
	V	19.99	19.83	19.14	15.63	−329.4	−2,555,047
Salehi Ahmad Abad et al. (CCC) [21]	*H*	0.011	3.06	9.172	22.145	504.104	4,258,491
	V	20.02	19.93	19.24	15.73	−328.86	−2,555,044
Analytical	*H*	0	3.060	9.172	22.146	504.103	4,258,491
	V	20.02	19.93	19.24	15.73	328.87	−2,555,044
Present	*H*	0	3.062	9.178	22.16	504.27	4,255,712
	V	20.03	19.94	19.25	15.74	−328.96	−2,553,369

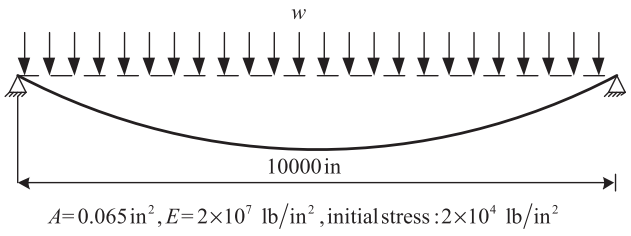

Fig. 9. Prestressed cable under uniform load.

Table 5
Results and comparison for prestressed cable under uniform load.

Load parameter	w (lb/in)	Mid-span displacement (in)			
		Elastic catenary [19]	Elastic parabola [41]	Analytical	Present
1	0.02	131.63	131.60	131.49	131.49
3	0.06	234.19	234.49	234.20	234.22
5	0.10	292.79	293.10	292.78	292.83
7	0.14	336.03	336.22	336.04	336.11
9	0.18	371.13	371.37	371.13	371.24

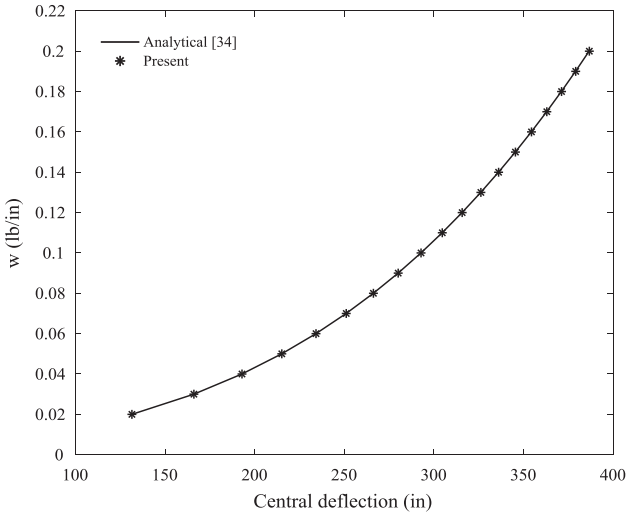

Fig. 10. Variation of central deflection with increasing weight for prestressed cable under uniform load.

Table 6
Comparison study for the longest cable of the Sutong Changjiang high-way bridge.

Researchers	Left $T_A(KN)$	Right $T_B(KN)$	Cable strained length P (m)	$Sag_{1/2}/P^*$
Ren & Gu [42]	7331.219	7114.005	576.616	1/101.725
Yang & Tsay [15]	7321.591	7104.359	576.616	1/101.236
Present	7327.549	7109.632	576.616	1/101.328

* Sag of the cable below the chord at $x = L/2$.

structure is shown in Fig. 11. The cross-sectional area, elastic modulus and self-weight per unit unstrained length of the cable are 146.45 mm^2, 82737 MPa and 1.459 N/m, respectively. Furthermore, inclined and horizontal cables maintain unstrained lengths of 30.419 m and 31.760 m, respectively. The problem was first studied by Saafan [40] and subsequently investigated by Jayaraman and Knudosn [19], Tibert [17] and Thai and Kim [18]. The internal nodes are subjected to a concentrated force of F_c = 35.586 kN. Each cable was modeled using a single elastic hyperbola element. Table 7 compares the present

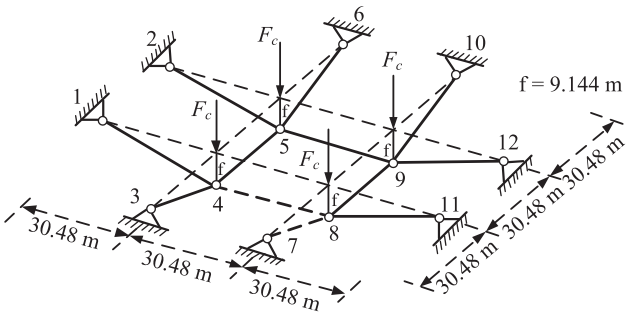

Fig. 11. Prestressed plane cable net.

Table 7
Comparison of displacements for node 4 in plane cable net.

Researcher(s)	Method	Displacement at node 4 (mm)		
		x-direction	y-direction	z-direction
Saafan [40]	Elastic straight	−40.35	−40.35	−448.27
Jayaraman & Knudson [19]	Elastic catenary	−39.62	−40.20	−446.32
Tibert [17]	Elastic catenary	−40.48	−40.48	−450.00
Tibert [17]	Associate catenary	−40.78	−40.78	−453.36
Tibert [17]	Elastic parabola	−40.78	−40.78	−453.36
Thai & Kim [18]	Elastic catenary	−40.13	−40.13	−446.50
Thai & Kim [18]	Elastic catenary (SAP2000)	−40.28	−40.28	−448.88
West & Kar [43]	Nonlinear equilibrium	−40.39	−40.39	−447.99
Present	Elastic hyperbola	−40.75	−40.75	−452.79

displacements for node 4 against those reported by other researchers. As it can be seen, the results are very close to previous studies. This implies that the proposed element provides satisfactory results in the static analysis of prestressed cable nets.

5.7. Hyperbolic paraboloid net

A hyperbolic paraboloid cable network is selected for which the experimental results are available in [44]. Various methods have been implemented by several researchers to numerically investigate this structure as well [14,18,28,44,45]. As shown in Fig. 12, the structure contains 31 cable segments pretensioned by the force of 200 N prior to the application of external loads. Some internal joints are subjected to concentrated loads of 15.7 N. All cables maintain an elastic modulus of 128.3 GPa and a cross-sectional area of 0.785 mm^2. A uniform weight per unit length equal to 0.195 N/m is assumed to act. The vertical displacements of this assembly are compared to the previous studies in Table 8. As it can be seen, the results predicted by the proposed scheme are in good agreement with those reported by the other researchers. It is

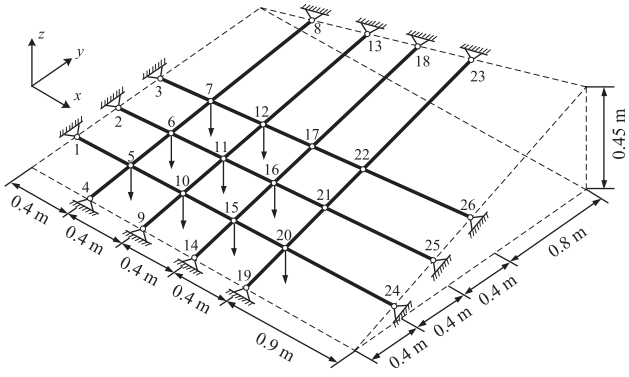

Fig. 12. Hyperbolic paraboloid net.

Table 8
Comparison of vertical displacements (mm) of hyperbolic paraboloid net.

Node	*Vertical displacement* (mm)						
	Experiment [44]	Dynamic Relaxation [44]	Minimum Energy [45]	Elastic catenary [18]	Approximation by series [28]	Elastic catenary [14]	Present
5	−19.50	−19.30 (1.03)*	−19.30 (1.03)	−19.56 (0.31)	−19.52 (0.10)	−19.51 (0.05)	−19.51 (0.05)
6	−25.30	−25.30 (0.00)	−25.50 (0.79)	−25.70 (1.58)	−25.35 (0.19)	−25.65 (1.38)	−25.58 (1.10)
7	−22.80	−23.00 (0.88)	−23.10 (1.32)	−23.37 (2.50)	−23.31 (2.24)	−23.37 (2.50)	−23.28 (2.10)
10	−25.40	−25.90 (1.97)	−25.80 (1.57)	−25.91 (2.01)	−25.86 (1.81)	−25.87 (1.85)	−25.83 (1.69)
11	−33.60	−33.80 (0.60)	−34.00 (1.19)	−34.16 (1.67)	−34.05 (1.34)	−34.14 (1.60)	−33.95 (1.04)
12	−28.80	−29.40 (2.08)	−29.40 (2.08)	−29.60 (2.78)	−29.49 (2.39)	−29.65 (2.95)	−29.42 (2.15)
15	−25.20	−26.40 (4.76)	−25.70 (1.98)	−25.86 (2.62)	−25.79 (2.34)	−25.86 (2.62)	−25.61 (1.62)
16	−30.60	−31.70 (3.59)	−31.20 (1.96)	−31.43 (2.71)	−31.31 (2.32)	−31.47 (2.84)	−31.02 (1.37)
17	−21.00	−21.90 (4.29)	−21.10 (0.48)	−21.56 (2.67)	−21.42 (2.00)	−21.57 (2.71)	−21.24 (1.12)
20	−21.00	−21.90 (4.29)	−21.10 (0.48)	−21.57 (2.71)	−21.48 (2.28)	−21.62 (2.95)	−20.83 (0.81)
21	−19.80	−20.50 (3.54)	−19.90 (0.51)	−20.14 (1.72)	−20.00 (1.01)	−20.15 (1.76)	−19.19 (3.08)
22	−14.20	−14.80 (4.23)	−14.30 (0.70)	−14.55 (2.46)	−14.40 (1.40)	−14.55 (2.46)	−13.81 (2.74)
‖Error‖		10.63	4.54	7.81	6.24	7.94	6.14

* Numbers in parentheses indicate the absolute error percentage with respect to experiment results.

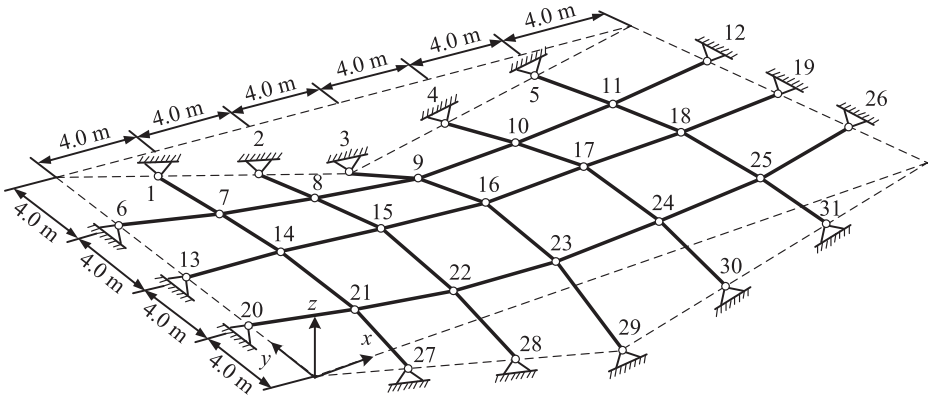

node No.	1	2	3	7	8	9	14	15	16
z coordinate (m)	-1.0000	-2.0000	-3.0000	-0.8195	-1.4096	-1.6769	-0.6770	-1.1478	-1.3176

Fig. 13. Spatial cable network.

Table 9
Comparison of displacements (mm) for spatial net.

Researcher	Direction	Displacements (mm)					
		Node					
		7	8	9	14	15	16
Lewis et al. [27] (Elastic straight)	*dx*	−5.14	−2.26	0.00	−4.98	−2.55	0.00
	dy	−0.42	−0.47	2.27	0.00	0.00	0.00
	dz	−30.41	−17.7	3.62	−43.49	−44.47	−41.65
Thai & Kim [18] (Elastic catenary)	*dx*	−5.03	−2.23	0	−4.92	−2.55	0.00
	dy	−0.41	−0.46	2.31	0.00	0.00	0.00
	dz	−29.86	−17.29	3.61	−42.85	−44.26	−42.08
Salehi Ahmad Abad et al. [21] (PCCC)	*dx*	−5.02	−2.24	0.00	−4.94	−2.56	0.00
	dy	−0.41	−0.43	2.23	0.00	0.00	0.00
	dz	−29.55	−17.55	3.19	−42.99	−44.30	−42.04
Salehi Ahmad Abad et al. [21] (PDCC)	*dx*	−5.05	−2.23	0.00	−4.93	−2.55	0.00
	dy	−0.40	−0.40	2.36	0.00	0.00	0.00
	dz	−29.55	−17.16	3.19	−42.94	−44.34	−42.14
Present (Elastic hyperbola)	*dx*	−5.03	−2.23	0.00	−4.93	−2.55	0.00
	dy	−0.40	−0.39	2.36	0.00	0.00	0.00
	dz	−29.50	−17.14	3.19	−42.94	−44.39	−42.20

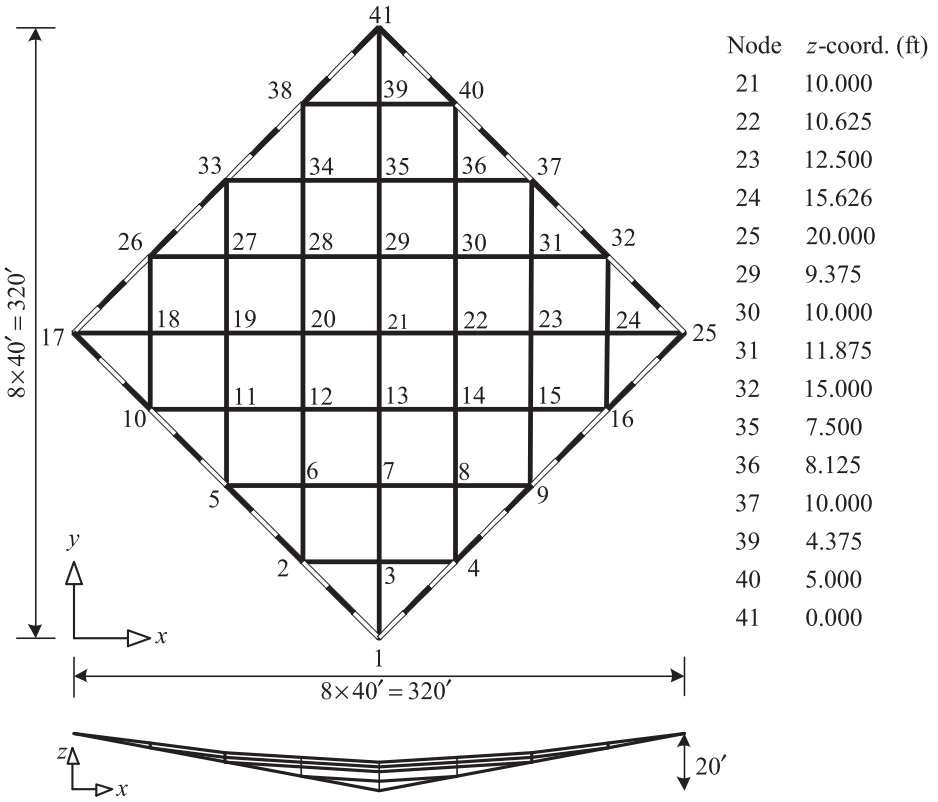

Fig. 14. Plan and side view of the pretensioned cable roof.

also drawn from this table that the present element leads to more satisfactory results in terms of the error norm compared to other techniques.

5.8. Spatial cable network

Another example examined here is a spatial cable network. The configuration of the structure is depicted in Fig. 13, in which symmetry about both centerlines is evident. The assembly is **24** m× 16 m in the plan, and 38 pretensioned cable segments have been used to divide its grid in 4 m× 4 m quadrilaterals. All cables maintain an elastic modulus of 160 GPa and the pretension force along the x and y directions are equal to 90 kN and 30 kN, respectively. All internal joints are subjected to a downward concentrated force of 6.8 kN. The cross-sectional areas of the cables along the x and y directions are also equal to 350 mm^2 and 120 mm^2, in a respective manner. A very small quantity is assumed for the cables' weight per unit length to carry out the analysis. The obtained displacements are compared to those reported by previous researchers in Table 9. As it can be seen, the proposed scheme leads to almost identical results.

5.9. Pretensioned cable roof

In this section, a pretensioned cable roof structure with symmetry about both centerlines is analyzed. The initial geometry and z coordinates for a quarter of the assembly are shown in Fig. 14. For the first time, this problem was introduced by Thornton and Birnstiel [46] and further studied by Ahmadi-Kashani [47]. The structure includes 64 pretensioned and weight-less cable segments. The side beams are assumed to be rigid. The horizontal component of the pretension force is 50 kips for all cables. The cross-sectional area and elastic modulus of the cables are given as 1 in^2 and 2.4 × 10^7 psi, respectively. Since the cables are assumed to be weight-less, a very small weight per unit volume of 10^{-6} $kips/ft^3$ is assigned to each element. The structure was analyzed for two different load cases. The first load case, indicated by LC.1, refers to a downward concentrated force of 1 kip applied to all joints. The second load case, denoted by LC.2, is similar to LC.1 plus an additional load of 14 kips applied at node 29. Table 10 compares the present vertical displacements of the sample joints against the benchmark results. As it can be seen, the results predicted by the proposed element are in excellent agreement with previous studies.

5.10. Suspended cable ring

This example serves to illustrate the efficiency of the proposed scheme in analysis of slack cable networks. The initial configuration of an axisymmetric suspended cable ring with inner radius of 35 m and outer radius of 75 m is presented in Fig. 15. The assembly consists of 8 radial and 8 tangential slack cable segments. The outermost joints are assumed to be fixed, while each of the inner joints maintains three

Table 10
Comparison of vertical displacements (ft) for example 9.

Node	*Vertical displacement* (ft)					
	LC. 1			LC. 2		
	Ahmadi-Kashani [47]	Thornton & Birnstiel [46]	Present	Ahmadi-Kashani [47]	Thornton & Birnstiel [46]	Present
1	0.00	0.00	0.00	0.00	0.00	0.00
3	−0.254	−0.254	−0.254	−0.259	−0.259	−0.259
7	−0.552	−0.552	−0.553	−0.605	−0.605	−0.606
13	−0.772	−0.772	−0.774	−1.020	−1.020	−1.023
21	−0.861	−0.861	−0.863	−1.722	−1.722	−1.727
29	−0.772	−0.772	−0.774	−3.720	−3.718	−3.727
35	−0.552	−0.552	−0.553	−1.268	−1.268	−1.272
39	−0.254	−0.254	−0.254	−0.381	−0.381	−0.381
41	0.00	0.00	0.00	0.00	0.00	0.00

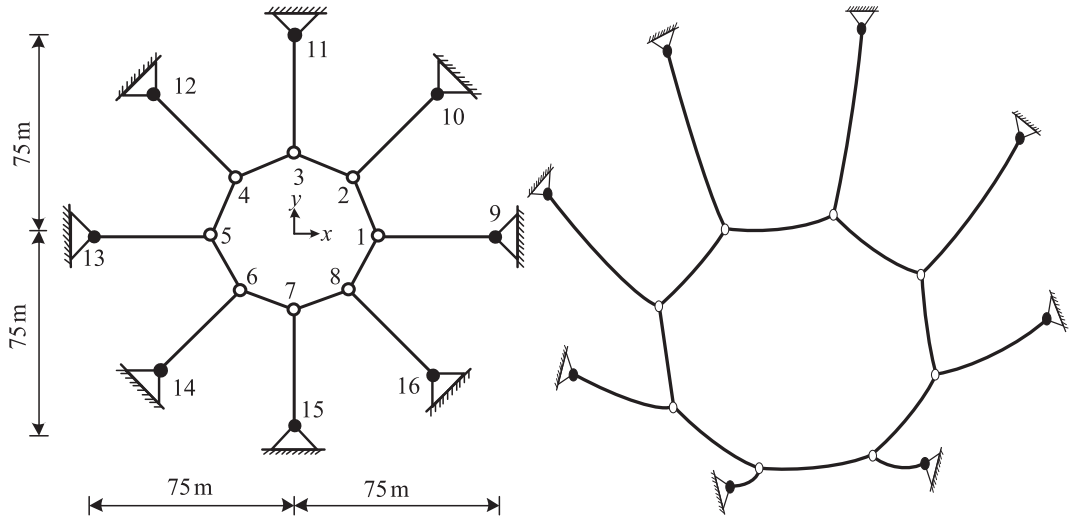

Fig. 15. Plan and perspective view of the suspended cable ring.

Table 11
Comparison of joint coordinates (m) at the final equilibrium state.

Researcher(s)	Direction (m)	Joint No.							
		1	2	3	4	5	6	7	8
Hüttner et al. [49]	x	41.469	29.451	0.000	−29.451	−41.649	−29.451	0.000	29.451
	y	0.000	29.451	41.469	29.451	0.000	−29.540	−41.649	−29.451
	z	−21.713	−21.713	−21.713	−21.713	−21.713	−21.713	−21.713	−21.713
Deng et al. [48]	x	41.469	29.451	0.000	−29.451	−41.649	−29.451	0.000	29.451
	y	0.000	29.451	41.469	29.451	0.000	−29.451	−41.649	−29.451
	z	−21.713	−21.713	−21.713	−21.713	−21.713	−21.713	−21.713	−21.713
Present	x	41.469	29.451	0.000	−29.451	−41.649	−29.451	0.000	29.451
	y	0.000	29.451	41.469	29.451	0.000	−29.451	−41.649	−29.451
	z	−21.717	−21.717	−21.717	−21.717	−21.717	−21.717	−21.717	−21.717

translational degrees of freedom. The cross-sectional area, elastic modulus and weight-per unit unstrained length of all cables are equal to $A = 1963.44\,\text{mm}^2$, $E = 170\,\text{GPa}$ and $w = 151.047\,\text{N/m}$, respectively. Further, the radial and tangential cables have unstrained lengths of 40 m and 32 m, respectively. The entire cable network is released from the initial state to deform under its self-weight. It is aimed to obtain the nodal coordinates of the final equilibrium state. Deng et al. used a rather arduous shape finding technique to solve this problem [48]. In this study, the analysis was simply carried out by modeling each cable segment with a single element. The coordinates of the inner joints at the final equilibrium state are compared to those reported by previous researchers in Table 11. As it can be seen, the proposed scheme has predicted identical results. This clearly indicates the reliability and applicability of the new formulation in shape finding and analysis of the slack cable structures.

6. Conclusions

Based on the concept of inextensible catenary, a novel formulation for three-dimensional cables was developed in this study. Authors' element is able to consider inclination without using any transformation matrices, takes the large sag effects into account, and it is applicable to the cables undergoing general load cases, such as, concentrated, uniformly distributed and thermal loads. The inextensibility condition was relaxed and equality of the total differentiation of the elastic elongation and strained length of the cable was employed to derive the explicit components of the tangent stiffness matrix. To trace the corresponding equilibrium paths of cable structures, the Newton-Raphson iterative method was also employed.

Unlike the elastic catenary approach, which requires a complicated iterative procedure for inverting the flexibility matrix and determination of three unknown nodal forces at each step, the proposed formulation leads to an explicit stiffness matrix. It has only one unknown force, namely the horizontal force. This makes the new element more efficient in terms of the analysis time. Significant case studies, ranging from single span cables to slack and pretensioned cable networks, were performed to illustrate the robustness of the present technique in analysis of various types of cable assemblies.

In addition to the simplicity and explicit nature of the equations and relations, the numerical outcomes clearly demonstrate that the proposed element furnishes accurate results and can be conveniently utilized in research, analysis and design of practical deep and shallow cable-supported structures such as pretensioned cable roofs, long-span cable stayed bridges and suspension bridges.

Declaration of conflicting interests

No potential conflicts of interest are declared by the authors with respect to the authorship, research and/or publication of this paper.

Funding

The authors received no financial supports either for the research or the authorship and publication of this article.

Appendix A

As it is given by Eqs. (20)–(28), the components of the tangent stiffness matrix are simplified using A_i and B_i constants. These constants are outlined below:

$$A_1 = (1-\alpha\Delta\vartheta)\frac{\sinh(\lambda)(\lambda L^2\cosh(\lambda)-l_y^2\sinh(\lambda))}{\lambda^2 l_x P} \tag{I.1}$$

$$A_2 = (1-\alpha\Delta\vartheta)\frac{l_y\sinh^2(\lambda)}{\lambda^2 P} \tag{I.2}$$

$$A_3 = (1-\alpha\Delta\vartheta)\frac{l_z}{P} \tag{I.3}$$

$$A_4 = -(1-\alpha\Delta\vartheta)\frac{2L^2}{l_x\lambda w P}\sinh(\lambda)(\lambda\cosh(\lambda)-\sinh(\lambda)) \tag{I.4}$$

$$A_5 = A_2\frac{l_x}{l_y} \tag{I.5}$$

$$A_6 = (1-\alpha\Delta\vartheta)\frac{\sinh(\lambda)(\lambda L^2\cosh(\lambda)-l_x^2\sinh(\lambda))}{\lambda^2 l_y P} \tag{I.6}$$

$$A_7 = A_3 \tag{I.7}$$

$$A_8 = A_4\frac{l_x}{l_y} \tag{I.8}$$

$$A_9 = A_5 \tag{I.9}$$

$$A_{10} = A_2 \tag{I.10}$$

$$A_{11} = (1-\alpha\Delta\vartheta)\frac{2H^2}{l_z w^2 P}(\lambda\sinh(\lambda)-2\sinh^2(\lambda)) + \frac{l_z}{P} \tag{I.11}$$

$$A_{12} = A_4\frac{l_x}{l_z} \tag{I.12}$$

$$\beta = \sqrt{\left(\frac{wl_z}{H\sinh(\lambda)}\right)^2 + 4} \tag{I.13}$$

$$\begin{aligned} B_1 = {} & \tfrac{1}{4\beta EAl_x\lambda\sinh(\lambda)}\{H\beta\sinh(\lambda)[\lambda L^2(\cosh(2\xi+4\lambda)+\cosh(2\xi)) \\ & - l_y^2(\sinh(2\xi+4\lambda)-\sinh(2\xi)) + 2\lambda(l_x^2-l_y^2)]-wl_z(\cosh(2\xi+4\lambda)-\cosh(2\xi))(\lambda L^2\coth(\lambda)-l_y^2)\} \end{aligned} \tag{I.14}$$

$$B_2 = \frac{l_y}{2EA}\left\{\frac{w}{4\lambda^2}(\sinh(2\xi+4\lambda)-\sinh(2\xi)+4\lambda)-\frac{Hl_z}{\beta L^2\sinh(\lambda)}(\cosh(2\xi+4\lambda)-\cosh(2\xi))\right\} \tag{I.15}$$

$$B_3 = \frac{H}{2EA\beta\sinh(\lambda)}(\cosh(2\xi+4\lambda)-\cosh(2\xi)) \tag{I.16}$$

$$B_4 = \frac{\lambda H}{\beta w^2 EAl_x\sinh(\lambda)}\{-\beta H\sinh(\lambda)[\lambda(\cosh(2\xi+4\lambda)+\cosh(2\xi))+\sinh(2\xi)-\sinh(2\xi+4\lambda)-2\lambda]-wl_z(\cosh(2\xi)-\cosh(2\xi+4\lambda))(\lambda\coth(\lambda)-1)\} \tag{I.17}$$

$$B_5 = B_2\frac{l_x}{l_y} \tag{I.18}$$

$$\begin{aligned} B_6 = {} & \frac{1}{4\beta EAl_y\lambda\sinh(\lambda)}\{H\beta\sinh(\lambda)[\lambda L^2(\cosh(2\xi+4\lambda)+\cosh(2\xi))-l_x^2(\sinh(2\xi+4\lambda)-\sinh(2\xi))+2\lambda(l_y^2-l_x^2)] \\ & -wl_z(\cosh(2\xi+4\lambda)-\cosh(2\xi))(\lambda L^2\coth(\lambda)-l_x^2)\} \end{aligned} \tag{I.19}$$

$$B_7 = B_3 \tag{I.20}$$

$$B_8 = B_4\frac{l_x}{l_y} \tag{I.21}$$

$$B_9 = \frac{l_x}{4\beta EAL\lambda\sinh(\lambda)}\{\beta H\sinh(\lambda)(\sinh(2\xi+4\lambda)-\sinh(2\xi)+4\lambda)-wl_z(\cosh(2\xi+4\lambda)-\cosh(2\xi))\} \tag{I.22}$$

$$B_{10} = B_9\frac{l_y}{l_x} \tag{I.23}$$

$$B_{11} = \frac{H}{2\beta EAwl_z \sinh(\lambda)}\{H\beta\sinh(\lambda)[\lambda(\cosh(2\xi + 4\lambda) + \cosh(2\xi)) - \sinh(2\xi + 4\lambda) + \sinh(2\xi) - 2\lambda] - wl_z(\cosh(2\xi + 4\lambda) - \cosh(2\xi))(\lambda\coth(\lambda) - 2)\} \tag{I.24}$$

$$B_{12} = -\frac{\lambda H}{\beta EAw^2 l_z \sinh(\lambda)}\{H\beta\sinh(\lambda)[\lambda(\cosh(2\xi + 4\lambda) + \cosh(2\xi)) - \sinh(2\xi + 4\lambda) + \sinh(2\xi) - 2\lambda] - wl_z(\cosh(2\xi + 4\lambda) - \cosh(2\xi))(\lambda\coth(\lambda) - 1)\} \tag{I.25}$$

Appendix B

The flowchart of the incremental Newton-Raphson solution procedure is given below:

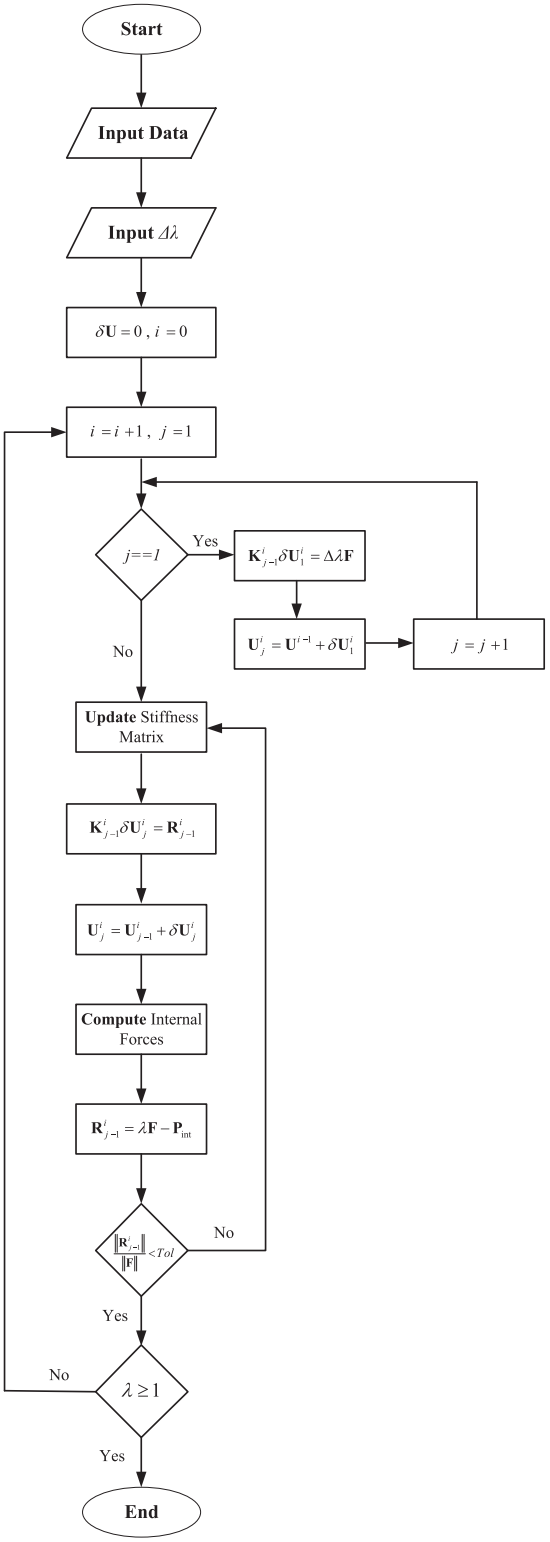

Appendix C. Supplementary material

Supplementary data associated with this article can be found, in the online version, at http://dx.doi.org/10.1016/j.engstruct.2018.04.022.

References

[1] Ernst JH. Der E-modul von seilen unter berucksichtigung des durchhanges. Der Bauingenieur 1965;40(2):52–5.
[2] Knudson WC. Static and Dynamic Analysis of Cable-net Structures. Berkeley: University of California; 1971.
[3] Liew JYR, Punniyakotty NM, Shanmugam NE. Limit-state analysis and design of cable-tensioned structures. Int J Space Struct 2001;16(2):95–110.
[4] Chen ZH, et al. Formulation and application of multi-node sliding cable element for the analysis of Suspen-Dome structures. Finite Elem Anal Des 2010;46(9):743–50.
[5] Gambhir ML, Batchelor Bde V. A finite element for 3-D prestressed cablenets. Int J Numer Meth Eng 1977;11(11):1699–718.
[6] Gambhir ML, Batchelor BD. Finite element study of the free vibration of 3-D cable networks. Int J Solids Struct 1979;15(2):127–36.
[7] Ozdemir H. A finite element approach for cable problems. Int J Solids Struct 1979;15(5):427–37.
[8] Coyette JP, Guisset P. Cable network analysis by a nonlinear programming technique. Eng Struct 1988;10(1):41–6.
[9] Ali HM, Abdel-Ghaffar AM. Modeling the nonlinear seismic behavior of cable-stayed bridges with passive control bearings. Comput Struct 1995;54(3):461–92.
[10] Wu JH, Su WZ. The non-linear finite element Analysis of cable structures based on four-node isoparametric curved element. J. Chongqing Jianzhu Univ. 2005;27(6):55–8.
[11] Wang Yang, Zuo SR, Wu C. A finite element method with six-node isoparametric element for nonlinear analysis of cable structures. Appl Mech Mater 2013;275–277:1132–5.
[12] Tang JM, Zhao Y, Wu LH. A Eeulerian geometrically non-linear finite element method with two node cable element for the analysis of cable structures. Shanghai J Mech 2005;21(1):89–94.
[13] Terence O'Brien W, Francis AS. Cable movements under two dimensional loads. J Structural Div ASCE 1964;90(3):89–124.
[14] Andreu A, Gil L, Roca P. A new deformable catenary element for the analysis of cable net structures. Comput Struct 2006;84(29):1882–90.
[15] Yang YB, Tsay J-Y. Geometric nonlinear analysis of cable structures with a two-node cable element by generalized displacement control method. Int J Struct Stab Dyn 2007;07(04):571–88.
[16] Ahmadi-Kashani K, Bell AJ. The analysis of cables subject to uniformly distributed loads. Eng Struct 1988;10(3):174–84.
[17] Tibert G. Numerical analyses of cable roof structures. in Trita-BKN. Bulletin. 1999, KTH: Stockholm. p. x, 180.
[18] Thai H-T, Kim S-E. Nonlinear static and dynamic analysis of cable structures. Finite Elem Anal Des 2011;47(3):237–46.
[19] Jayaraman HB, Knudson WC. A curved element for the analysis of cable structures. Comput Struct 1981;14(3):325–33.
[20] Pevrot AH, Goulois AM. Analysis of cable structures. Comput Struct 1979;10(5):805–13.
[21] Salehi Ahmad Abad M, et al. Nonlinear analysis of cable structures under general loadings. Finite Elem Anal Des 2013;73(1):11–9.
[22] Naghavi Riabi AR, Shooshtari A. A numerical method to material and geometric nonlinear analysis of cable structures. Mech Based Des Struct Mach 2015;43(4):407–23.
[23] Crusells-Girona M, Filippou FC, Taylor RL. A mixed formulation for nonlinear analysis of cable structures. Comput Struct 2017;186(Supplement C):50–61.
[24] Gimsing NJ, Georgakis CT. Cable Supported Bridges: Concept and Design. Wiley; 2011.
[25] Gründig L, Bahndorf J. The design of wide-span roof structures using micro-computers. Comput Struct 1988;30(3):495–501.
[26] Haber RB, Abel JF. Initial equilibrium solution methods for cable reinforced membranes part I—formulations. Comput Methods Appl Mech Eng 1982;30(3):263–84.
[27] Lewis WJ. The efficiency of numerical methods for the analysis of prestressed nets and pin-jointed frame structures. Comput Struct 1989;33(3):791–800.
[28] Kwan ASK. A new approach to geometric nonlinearity of cable structures. Comput Struct 1998;67(4):243–52.
[29] Stefanou GD, Nejad SEM. A general method for the analysis of cable assemblies with fixed and flexible elastic boundaries. Comput Struct 1995;55(5):897–905.
[30] Hüttner M, Máca J, Fajman P. The efficiency of dynamic relaxation methods in static analysis of cable structures. Adv Eng Softw 2015;89(Supplement C):28–35.
[31] Bouaanani N, Marcuzzi P. Finite difference thermoelastic analysis of suspended cables including extensibility and large sag effects. J Therm Stresses 2011;34(1):18–50.
[32] Bouaanani N, Ighouba M. A novel scheme for large deflection analysis of suspended cables made of linear or nonlinear elastic materials. Adv Eng Softw 2011;42(12):1009–19.
[33] Choi D-H, Gwon S-G, Na H-S. Simplified analysis for preliminary design of towers in suspension bridges. J Bridge Eng 2014;19(3):04013007.
[34] Riks E. The application of newton's method to the problem of elastic stability. J Appl Mech 1972;39(4):1060–5.
[35] Mondkar DP, Powell GH. Evaluation of solution schemes for nonlinear structures. Comput Struct 1978;9(3):223–36.
[36] Powell G, Simons J. Improved iteration strategy for nonlinear structures. Int J Numer Meth Eng 1981;17(10):1455–67.
[37] Padovan J, Tovichakchaikul S. Self-adaptive predictor-corrector algorithms for static nonlinear structural analysis. Comput Struct 1982;15(4):365–77.
[38] Irvine HM. Cable Structures. 1992: Dover Publications.
[39] Michalos J, Birnstiel C. Movements of a cable due to changes in loading. J Struct Div 1960;86(12):23–38.
[40] Saafan SA. Theoretical Analysis of Suspension Roofs. Journal of the Structural Division, 1970. 96(2): p. 393.405.
[41] Wei-Xin R, Meng-Gang H, Wei-Hua H. A parabolic cable element for static analysis of cable structures. Eng Comput 2008;25(4):366–84.
[42] Ren SY, and Gu MJ. Static analysis of cables configuration in cable stayed bridges. Tongji Uni. (Nat. Sci.), 2005. 33(5): p. 595–599.
[43] West HH, Kar AK. Discretized initial-value analysis of cable nets. Int J Solids Struct 1973;9(11):1403–20.
[44] Lewis WJ, Jones MS, Rushton KR. Dynamic relaxation analysis of the non-linear static response of pretensioned cable roofs. Comput Struct 1984;18(6):989–97.
[45] Sufian FMA, Templeman A. On the non-linear analysis of pre-tensioned cable net structures. Struct Eng 1992;4:147–58.
[46] Charles H. Thornton and C. Birnstiel, Three-Dimensional Suspension Structures. Journal of the Structural Division, 1967. 93(2): p. 247–270.
[47] Ahmadi-Kashani K. U.o.M.I.o. Science, and Technology, Development of Cable Elements and Their Applications in the Analysis of Cable Structures. 1983: University of Manchester Institute of Science and Technology (UMIST).
[48] Deng H, Jiang QF, Kwan ASK. Shape finding of incomplete cable-strut assemblies containing slack and prestressed elements. Comput Struct 2005;83(21):1767–79.
[49] Hüttner M, Máca J, and Fajman P. Numerical Analysis of Cable Structures. Proceedings of the Eleventh International Conference on Computational Structures Technology, Civil-Comp Press, Stirlingshire, Scotland, 2012.